

Automatic calibration of LDA measurement volume size

Mark Saffman

The problem of particle number density measurements with a laser Doppler anemometer is addressed. Analytical expressions for the instrument measurement cross section are given. An automatic calibration method for determining unknown scattering parameters, which promises good accuracy in changeable optical conditions, is described. Estimates of the measurement uncertainty are derived and the method is extended to uses in 2-D flow fields.

I. Introduction

Laser Doppler anemometry (LDA) is a well-established diagnostic for nonintrusive fluid flow measurements. The method can also be extended to include particle size measurements using various techniques,¹⁻⁴ such as signal intensity, modulation depth, or phase. In many uses it is also necessary to measure particle number density, which requires knowledge of the instrumental measurement volume size. Due to the Gaussian light distribution of laser beams, the variation of scattering cross section with particle size and optical losses caused by variable measurement conditions, accurate number density measurements are difficult and have rarely been reported in the literature.

A new method of automatically determining the measurement volume on-line without the necessity of calibrating with known particle sizes and/or number densities is described. The method dynamically adapts to changing measuring conditions and is generally adaptable to any type of combined LDA particle sizing instrument, although it will be described in connection with the phase method of particle sizing.

The optical geometry is described followed by a brief review of previous calibration methods and a description of an automatic method based on burst length measurements. A number of potential error sources are identified, error bounds are given, and it is shown how the method can be modified for measurements of 2-D flow fields.

II. Optical Geometry

The optical geometry of the LDA measurement volume is shown in Fig. 1. The intersection of the crossing region of the two incident laser beams and the region which is imaged onto the collection optics spatial filter defines the measurement volume. The light intensity distribution in the measurement volume is a sinusoidal interference pattern with an envelope which, to a good approximation, is a Gaussian function of the radial distance and a Lorentzian along the beam bisector. We take a collection direction perpendicular to the bisector of the incident beams and use a spatial filter in the form of a narrow slit parallel to the X axis and can therefore neglect the light intensity variation along the Z axis.

With the assumption of 1-D flow along the X axis the problem of determining the measurement volume reduces to finding the measurement cross section perpendicular to the X axis, and the particle number density is given by

$$\text{rho}(D) = R(D)/[U(D)A(D)], \quad (1)$$

where rho , R , U , and A are, respectively, the number density per unit volume [$\#/M^{**3}$], the data rate per second [$\#/s$], the velocity [M/s], and the measurement cross-sectional area [M^{**2}], all of which are functions of the particle diameter. R and U are measured and it remains to determine $A(D)$. It is apparent that Eq. (1) is valid only when the number density and measurement volume are such that individual particles are detected, i.e., there is small probability of multiple probe volume occupancy.

The signal level and duration due to a single particle passing the measurement volume depend on the laser power, test cell optical losses, particle density, system geometry, electronic gain, particle size, shape, refractive index, and trajectory. The incident light level decreases as the particle trajectory moves away from the center of the measurement volume, and the parti-

The author is with Dantec Elektronik, DK-2740 Skovlunde, Denmark.

Received 23 October 1986.

0003-6935/87/132592-06\$02.00/0.

© 1987 Optical Society of America.

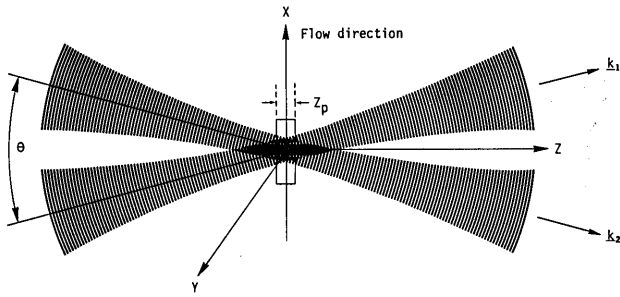


Fig. 1. Measurement volume geometry.

cle scattering cross section increases as the particle size increases so that the area giving usable signals increases with particle size. Accurate measurements of relative size distributions require correction for the size-dependent cross-sectional bias, and absolute number density measurements require absolute knowledge of the cross-sectional area. The envelope of the electronic signal due to a particle of diameter D at position x, y can be written

$$V(D, x, y) = G * s(D) * I_0 \exp\{-[8y^2/d_y^2 + 8x^2 \cos^2(\theta/2)/d_y^2]\}, \quad (2)$$

where θ is the beam crossing angle, d_y is the Gaussian spot diameter, I_0 is the incident intensity at $x = y = 0$, $s(D)$ is a generalized scattering cross section that depends on the particle characteristics and size and the position and size of the collection aperture, and G is an electronic gain factor accounting for detector quantum efficiency and detector and amplifier gains. With our assumption of 1-D flow the x coordinate is related to the particle velocity by $x = U(t - t_0)$ where t_0 is the time when the particle passes the y - z plane.

Electronic processors used for LDA measurements in situations where the probability of multiple occupancy of the measurement volume is low (sparsely seeded flows) typically include a circuit generically known as a burst detector. The burst detector determines when a signal is present which the rest of the instrument can analyze for velocity and size information. Burst detectors, which are used with counter type LDA processors, generally require a minimum number of signal periods above a fixed trigger level. We denote the trigger level as V_t and the required number of signal periods as N_0 , so the condition for a signal of sufficient amplitude and duration is

$$V_t \leq V_m(D) \exp\{-[8y^2/d_y^2 + 2(N_0/N_f)^2]\}, \quad (3)$$

where $V_m(D) = Gs(D)I_0$ is the maximum signal level at the center of the burst and $N_f = \cos(\theta/2)d_y/d_f$ is the number of fringes inside the Gaussian envelope (d_f being the fringe spacing). We note that if the number of signal periods greatly exceeds N_0 , the particle will still only be measured once due to logical checks in the burst detector circuitry. The maximum trajectory displacement y_m can then be solved for as

$$y_m(D) = (d_y/2\sqrt{2}) \{\ln[V_m(D)/V_t] - 2(N_0/N_f)^2\}^{1/2}, \quad (4)$$

and the measurement cross section is given by

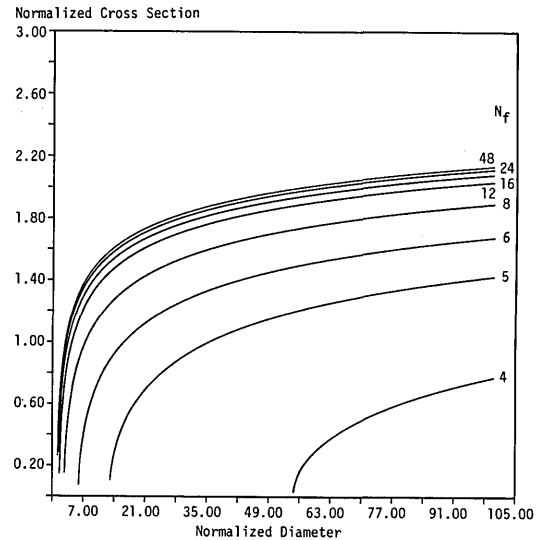


Fig. 2. Family of curves showing the dependence of cross section on diameter. The parameters are defined in the text and the curves are labeled with the value of N_f .

$$A(D) = 2 * z_p * y_m(D) \\ = (z_p d_y / \sqrt{2}) * \{\ln[V_m(D)/V_t] - 2(N_0/N_f)^2\}^{1/2}, \quad (5)$$

where z_p is the length along the Z axis of the image of the collection optics spatial filter. All the parameters in the expression for the cross section are known from the optical and electronic system parameters except for $V_m(D)$ which must be measured. To get a feeling for how the burst length and cross section vary with particle size we can assume $V_m(D) \sim D^2$, which gives the family of curves shown in Fig. 2. The normalized diameter is D/D_0 , where $V_m(D_0) = V_t$, the normalized cross section is $A(D)/z_p d_y$, and we have set $N_0 = 8$. We note that, if it is desired to reduce the dependence on the particle diameter, N_f/N_0 should be greater than ~ 1.5 and $[V_m(D)]/V_t$ should be greater than ~ 100 . The last requirement is generally not practical and there will be a noticeable bias in favor of the larger particles.

III. Previous Calibration Methods

It has been recognized for many years that optical, particle, and electronic parameters all interact to determine the cross-sectional size (see, for example, Refs. 5 and 6) and formulas equivalent to Eq. (5) have been derived previously. The formula has typically been implemented in one of two ways.

The cross-sectional area which gives accepted signals can be directly measured using a wire or other scattering center mounted on a traversing stage. At the same time a calibration value of V_m can be measured. The change in V_m , which should be used when measuring in a flow field, can then be estimated analytically taking account of changes in particle characteristics and optical conditions, and Eqs. (1) and (5) can then be used for absolute measurements.

Alternatively, if a monodisperse flow with a known number density and particle size is available this can

be used as a calibrating device for the cross section using Eq. (1). The change in cross section for other particle sizes can then be analytically determined based on Mie scattering calculations or by simply assuming a scattering cross section proportional to the particle diameter squared.

In principle these methods can be used as a basis for accurate measurements. In practice they require inordinate care on the part of the experimentalist, precise definition of the optical geometry, and very careful attention to changes between laboratory and field measurement conditions. Well-documented measurements of number densities, in flow fields with large variations in particle size, have, to the authors' knowledge, not been reported.

IV. Automatic Calibration Method

To overcome these practical difficulties an *in situ* automatic calibration method is required. Such a method should be based as little as possible on analytic models and as much as possible on the actual signals detected. If this is the case it should also be possible to account for changing optical conditions during a measurement. Number density measurements using a method presumably similar to that described in the following have recently been reported⁷ although no details are given.

Looking back at Eq. (5) the only unknown parameter is $V_m(D)$. If this could be determined *in situ* based on the actual measured signals, Eq. (5) could be reliably used. The immediate difficulty is that only $V(D,x,y)$ or $V'(D,y) = V(D,x = 0,y)$, the maximum amplitude at the center of the burst, which depends on the particle trajectory, can be directly measured. However, the distribution of the measured values of V' can be statistically related to the actual value of $V_m(D)$. If the size measurement is independent of the signal amplitude, such as is the case with the phase method, and if the dimensions of the measurement cross section are smaller than the characteristic dimensions over which the flow field changes significantly so that a particle has equal probability of crossing any part of the measurement cross section, the measured V' values can be directly averaged without any additional, unknown weighting function.

The unknown value of V_m can then be related to the measured average value of V' using Eqs. (2) and (4). Unfortunately the averaging process gives results proportional to error function integrals so there is no simple closed form solution for V_m . The problem can be solved by measuring the average value of V' and then relating V_m to the percentage of the measurements which are greater than or less than the average value. This works but requires a larger number of measurements for good statistical accuracy than would direct use of the average value. Furthermore, the requirement on the dynamic range of the electronics is stringent since for a particle diameter variation of 40 the signal can vary by a factor of up to 1600.

There is an alternative approach which is more easily implemented and can be solved in closed form. The

burst length can be defined geometrically as the number of signal periods above the burst detector trigger level multiplied by the fringe spacing. This can be expressed as

$$L(D,y) = (d_p/\sqrt{2} \cos(\theta/2)) * \{\ln[V_m(D)/V_t] - 8y^2/d_p^2\}^{1/2}. \quad (6)$$

The average value of the measured burst lengths can then be used to give V_m . This again gives algebra which cannot be solved in closed form but if we average over the burst length squared we have

$$\langle L^2(D) \rangle = (1/y_m) \int L^2(D,y) dy \quad (7)$$

$$= (1/3) [d_p^2/\cos^2(\theta/2)] \{\ln[V_m(D)/V_t] + (N_0/N_p)^2\}. \quad (8)$$

Solving for V_m and using Eq. (5) then gives

$$A(D) = (3/2)^{1/2} z_p d_p \{\cos^2(\theta/2) [\langle L^2(D) \rangle / d_p^2] - (N_0/N_p)^2\}^{1/2}. \quad (9)$$

This is the basic result for *in situ* cross-sectional calibration. We note that since we now average over burst length the method can also be used with sizing techniques that depend on the signal amplitude and, since $A(D)$ does not explicitly depend on D , the number density of monodisperse flows can be measured without knowledge of the particle size.

The method automatically accounts for changing optical conditions during a measurement in the following sense. Consider, for example, some flow in a test cell where the windows become progressively dirtier during the measurement. This has two effects: $R(D)$ will be reduced due to the reduced signal levels and hence smaller number of accepted signals, and $\langle L^2(D) \rangle$ will also be reduced. These two quantities appear in both the numerator and denominator of Eq. (1) so the effects should tend to cancel out, provided the number of measurements is sufficient to give a good statistical estimate of $\langle L^2(D) \rangle$. The requirement on the number of measurements will be evaluated below.

V. Error Estimates

We derive here estimates for the accuracy of this type of number density measuring technique. The relevance of such error or uncertainty estimates will depend on the measurement conditions, signal quality, care taken by the experimentalist, etc. It is only possible to make precise predictions of the measurement uncertainty by referring explicitly to a specific measurement situation. The intention of this section is to show that it is possible to obtain rms uncertainties of the order of 10% in realistic conditions and to estimate the number of measurements necessary for good statistical accuracy.

The number density which is defined by Eq. (1) is a function of three independent parameters. Each of these parameters has various uncertainties associated with it, although the highest uncertainty level will invariably be associated with the measurement cross section. The particle arrival rate R can be assumed to be accurately measured provided that the inverse of the instrument dead time associated with a single measurement is much larger than the mean particle arrival rate. Furthermore, since the particle arrival statistics

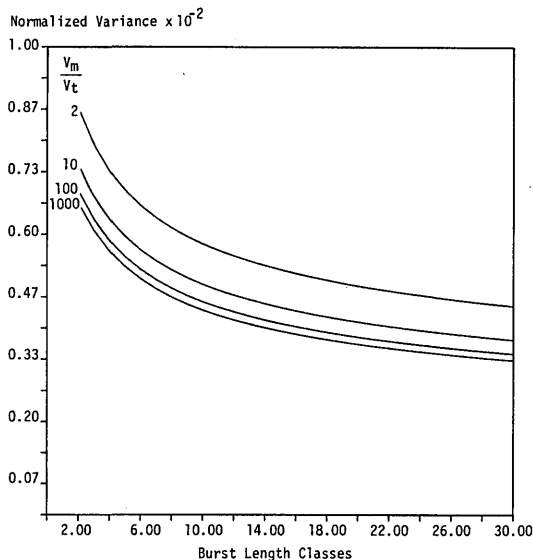


Fig. 3. Normalized variance of the burst length measurement as a function of the number of burst length classes.

are generally Poisson distributed, the number of particles counted in each size class should be at least 100 for 10% accuracy. The velocity is typically measured to an accuracy of several percent when using a LDA in favorable conditions and is not an important error source in this connection.

The cross section as described by Eq. (9) depends on five independent parameters, N_0 , θ , d_y , z_p , and $\langle L^2 \rangle$, which are listed in an order indicating increasing levels of uncertainty. (N_f is not independent if θ and d_y are known, since the laser wavelength is always known to a very high accuracy.) The uncertainties associated with each of these parameters will now be briefly described. The number of signal periods required by the burst detector is very well defined electronically and, provided the signal-to-noise ratio is good, this condition will be met by all the accepted signals. For low signal-to-noise ratios the effective value of N_0 will tend to fluctuate and increase the measurement uncertainty. The beam crossing angle is well defined by the optical setup and can be easily measured to a few percent accuracy, or to a very high accuracy with a good deal of effort. The Gaussian spot diameter depends on the beam diameter of the laser being used and on the relay and focusing lenses in the optical system. Laser manufacturers typically specify the beam diameter to better than 10% accuracy, and if care is taken in placing the beam waist at the beam crossing point, the spot size will also be known to about this accuracy. Alternatively the spot size can be easily measured with commercial beam scanning devices to an accuracy of just a few percent. The effective axial length of the collection optics spatial filter is well defined, given the magnification of the collection optics, but there will always be a blurry region at the edges of the area defined by the spatial filter giving some uncertainty as to the effective size. With a spatial filter of characteristic dimension (100 μm), the blurry region can in any

case be restricted to a <5% effect. We have also assumed that the light intensity does not vary with the z coordinate. This will be determined by the ratio of z_p to the length of the intensity envelope along the z axis. If we match z_p to the spot diameter d_y , the ratio of z_p to the z envelope length is given approximately by $\sin\theta/2$. If θ does not exceed 20° , which is almost always the case in practice, the intensity will only have fallen by $\sim 6\%$ at $z = z_p/2$, which gives an error of similar size to the other uncertainties.

The remaining parameter is $\langle L^2 \rangle$ which is measured in a statistical sense. To ensure a good estimate of $\langle L^2 \rangle$, all parts of the measurement cross section must be sampled, i.e., a large number of particles must be measured. Since the value of L^2 decreases quadratically with the trajectory offset y , equal intervals in L correspond to progressively smaller intervals in y , and the requirement on the number of measurements per size class for a desired statistical uncertainty should be checked. We approximate Eq. (7) by

$$\begin{aligned} \langle L^2 \rangle &= (1/N) \sum L_i^2 n_i \\ &= (1/N) \sum L^2(y_i) n(y_i) \\ &= (\delta L / y_m) \sum L^2(y_i) 1 / (\partial L / \partial y | y_i). \end{aligned} \quad (10)$$

Where we have used $n(y_i) = N \delta y_i / y_m$, the $\delta y_i = \delta L / (\partial L / \partial y | y_i)$, δL is the spread in L per measured class, and $N = \sum n_i$ is the number of measurements with diameter D . The normalized variance of the burst length measurement can then be written as

$$\sigma^2 / \langle L^2 \rangle^2 = (1/N) \frac{\sum L^4(y_i) 1 / (\partial L / \partial y | y_i)}{[\sum L^2(y_i) 1 / (\partial L / \partial y | y_i)]^2}. \quad (11)$$

Here we have assumed Poisson particle arrival statistics so the variance of the number of particles in each burst length class is given by the expected mean. Equation (11) can be evaluated by assuming a fixed number of classes and approximating the summations by integrals, using Eq. (6) for $L(y)$. The results, expressed as a normalized variance vs the number of burst length classes, are shown in Fig. 3 for $N = 100$ and $N_0 / N_f = 0.5$. We see that the uncertainty decreases as the number of burst length classes and V_m / V_t increase and that 100 measurements per size class is sufficient for <10% uncertainty. Since flows with a wide size distribution may require up to 100 size classes for good resolution, we need the order of 10,000 measurements to accurately characterize the flow at a single point in space.

VI. Extension to 2-D Flows

In many uses the particle velocity is a 2-D or 3-D vector quantity, and it is not sufficient to consider only the component parallel to the x axis. In general the relationship between burst length L and V_m [Eq. (6)] must be modified to take account of the trajectory direction. To keep the algebra compact and because it is sufficient for a large number of applications, we restrict ourselves to 2-D velocities in the x - y plane.

If we consider again the distribution of trajectories throughout the measurement cross section, there are

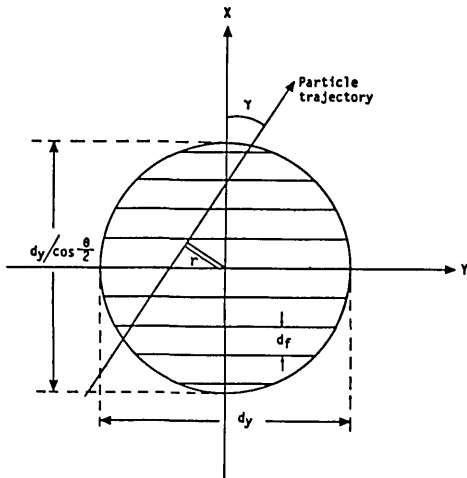


Fig. 4. Two-dimensional trajectories.

now two parameters that must be averaged over for each size class. These are shown in Fig. 4 as r , the radial trajectory offset from the point $x = y = 0$, and γ , the angle which the trajectory makes with the x axis. If the measuring system includes a second channel for measurement of the y velocity component, γ can be determined for each burst, although r will be unknown and must be statistically averaged over, as with the y coordinate in the 1-D case. Each particle size will have a mean angle γ with a finite spread associated with it. In principle, the variation in r for each measured γ could be averaged over, although the statistical uncertainty will be high for the extreme γ values which only occur a few times. We take the simpler approach of measuring the mean value for each size class, $\gamma(D)$, and then averaging over r .

Despite the restriction to 2-D velocities the exact expression for the burst length as a function of γ and r is algebraically complicated,⁸ and it does not appear possible to obtain a simple expression equivalent to Eq. (8). Therefore we simplify the problem again. For the trajectory with $r = 0$ the burst length is

$$L(D, \gamma) = (d_y / \sqrt{2}) \{ [1 / \{\tan^2 \gamma + \cos^2(\theta/2)\}]^{1/2} \ln[V_m(D) / V_i] \}^{1/2}, \quad (12)$$

which is simply Eq. (6) with an additional factor accounting for the variation in the number of fringes crossed with $\cos \gamma$ and for the slight ellipticity of the Gaussian intensity contour due to the factor $\cos \theta/2$. We approximate the dependence on r by making the substitution $y^2/d_y^2 \rightarrow (r^2/d_y^2)(\sin^2 \gamma \cos^2(\theta/2) + \cos^2 \gamma)$ which gives

$$L(D, \gamma, r) = (d_y / \sqrt{2}) \{ [1 / \{\tan^2 \gamma + \cos^2(\theta/2)\}]^{1/2} \times \{ \ln[V_m(D) / V_i] - (8r^2/d_y^2) [\sin^2 \gamma \cos^2(\theta/2) + \cos^2 \gamma] \}^{1/2} \} \quad (13)$$

The maximum trajectory displacement can then be solved for as

$$r_m(D, \gamma) = \{ d_y / 2\sqrt{2} [\sin^2 \gamma \cos^2(\theta/2) + \cos^2 \gamma]^{1/2} \times \{ \ln[V_m(D) / V_i] - 2(N_0/N_f)^2 [1 + \tan^2 \gamma / \cos^2(\theta/2)] \}^{1/2} \} \quad (14)$$

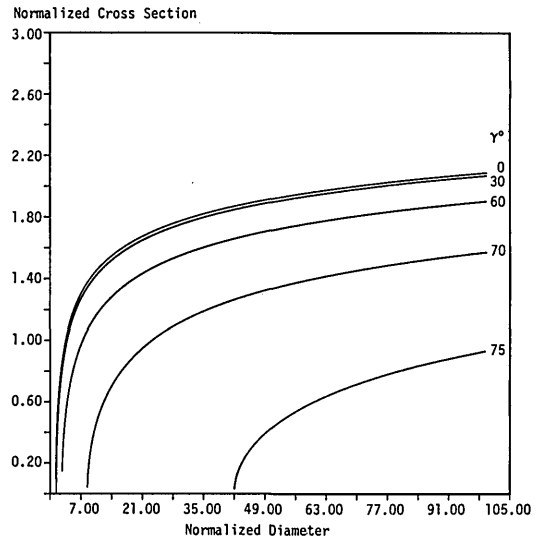


Fig. 5. Family of curves showing the dependence of cross section on diameter for 2-D trajectories. The parameters are as in Fig. 2 with $N_f = 16$ and the curves are labeled with the value of γ .

We then compute the expected average of L^2 , solve for $V_m(D)$, and use Eq. (14) to give

$$A(D, \gamma) = 2 * z_p^* r_m(D, \gamma) = (3/\sqrt{2}) z_p d_y \{ [\cos^2(\theta/2) + \tan^2 \gamma] / [\cos^2(\theta/2) \times \{ \sin^2 \gamma \cos^2(\theta/2) + \cos^2 \gamma \}] \}^{1/2} \times \{ \cos^2(\theta/2) [L^2(D, \gamma) / d_y^2] - (N_0/N_f)^2 \}^{1/2} \quad (15)$$

for the cross section as a function of the diameter and the trajectory angle. As a partial check on the algebra we see that the result reduces to Eq. (9) for $\gamma = 0$. The dependence on γ is shown in Fig. 5 for $N_0/N_f = 0.5$. We see that for angles greater than $\sim 30^\circ$ there is a very large reduction in the cross section. If the flow angle is correlated with the particle size, a bias will be introduced in the measured distribution unless this effect is accounted for.

VII. Conclusions

We have examined the problem of number density measurements with a LDA. It is shown that such measurements can be accurately made if an optical measurement cross section can be defined. Simple geometric expressions for the cross section, which include an unknown scattering function, are derived. It is pointed out that previous work has suffered from the difficulties associated with measuring the unknown scattering function. A new approach is described which allows the unknown parameter to be statistically measured *in situ* without the need for independent calibration.

The method is shown to automatically adapt to variable optical conditions and promises reliable results in difficult conditions where the particle size distribution is very broad.

References

1. W. M. Farmer, "Measurement of Particle Size, Number Density, and Velocity Using a Laser Interferometer," *Appl. Opt.* 11, 2603 (1972).
2. P. Buchhave, J. Knuhtsen, and P. E. Oildag, "A Laser Doppler Apparatus for Determining the Size of Moving Spherical Particles in a Fluid Flow," International Patent Application PCT/DK83/00054 (1983).
3. M. Saffman, P. Buchhave, and H. Tanger, "Simultaneous Measurement of Size, Concentration, and Velocity of Spherical Particles by a Laser Doppler Method," in *Proceedings, Second International Symposium on Applications of Laser Anemometry to Fluid Mechanics*, Lisbon (1984).
4. L. E. Drain, "Laser Anemometry and Particle Sizing," in *Proceedings, International Conference on Laser Anemometry—Advances and Applications*, Manchester (1985).
5. W. M. Farmer, "Sample Space for Particle Size and Velocity Measuring Interferometers," *Appl. Opt.* 15, 1984 (1976).
6. E. D. Hirleman, S. L. K. Wittig, and J. V. Christiansen, "Development and Application of an Optical Exhaust Gas Particulate Analyzer," Report RE 76-4, Laboratoriet For Energiteknik, Technical University of Denmark (1976).
7. W. D. Bachalo and M. J. Houser, "An Instrument for Two-Component Velocity and Particle Size Measurement," in *Proceedings, Third International Symposium on Applications of Laser Anemometry to Fluid Mechanics*, Lisbon (1986).
8. P. Buchhave, "Biasing Errors in Individual Particle Measurements with the LDA-Counter Signal Processor," in *Proceedings, LDA-Symposium*, Copenhagen (1976).

Patter continued from page 2553

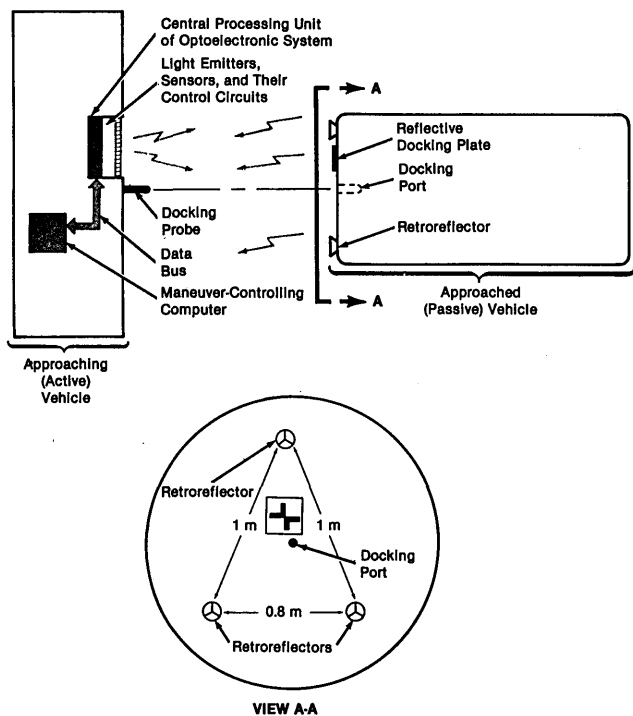


Fig. 1. Optoelectronic docking system automatically controls the approach of an active vehicle or mechanism to a passive vehicle or object. The maneuvers of the approaching vehicle are controlled in response to the optoelectronically sensed relative position of the approached vehicle.

the distance to the target is determined from the time of flight of the light pulses; the approach speed is calculated from the rate of change of the distance.

At a distance of 30 m, the approach-control task is handed to a cw laser tracking subsystem, which distinguishes among the return signals from the three retroreflectors. In this case, the 20° by 20° field of view is still scanned by driving twenty transmitting and twenty receiving diodes in sequence, but the three target returns are detected in separate diodes, and the distance (within about ± 3 cm) to each retroreflector is computed by measurement of the relative

phase, in the return signal, of a 3-MHz modulation imposed on the transmitted signal. From the three range signals, the system computes the average target distance and the orientation of the target relative to the line of sight. The coordinates of the return signals are also processed to compute both the direction to the target and the target roll angle and roll rate.

A charge-coupled-device-TV/pulse-ranging system takes over at distances of less than 3 m: from 3 m to 1 m, the system processes the outline of the reflective docking plate in the TV image to determine the target pitch and yaw; at 1 m, the docking-plate image exceeds the camera field of view and the system begins to seek alignment between four laser beams and the converging edges of the dark pattern in the docking plate; at a distance of 35 cm, the docking probe enters the docking port; and at 20 cm, the probe closes a hard-docking indicator switch, which deactivates the system.

This work was done by Steven M. Ward of Energy Optics, Inc., for Johnson Space Center. For further information, refer to MSC-21159.

Sliding capacitive displacement transducer

A sliding capacitive displacement transducer, the capacitance of which varies linearly with displacement, enables the use of a simple circuit based on an operational amplifier instead of a more complicated capacitance bridge. With the new circuit, transducers as small as 1.3 mm square and 0.1 mm thick have produced output-voltage changes of ~ 200 mV/0.13 mm of displacement. Examples of transducers and the circuit are shown in Fig. 2. The flat-plate transducer is sensitive only to motion in the x direction, since motion in the y direction does not change the area of overlap. The piston-type transducer can be made quite small for installation in confined spaces.

The circuit includes a charge amplifier, consisting of an operational amplifier with a stable fixed capacitor in its feedback loop. When an alternating voltage of fixed amplitude is applied to the capacitive transducer, the amplitude of the output of the charge amplifier changes by an amount proportional to the change of capacitance produced by the motion of the displacement transducer. The detector rectifies the amplifier output, producing a voltage that changes by an amount proportional to the change in capacitance and, therefore, to the displacement. To adjust the final output signal to zero for some selected reference displacement, a steady voltage equal to the signal voltage at that displacement is subtracted from the signal. Once that has been done, the final output voltage will be proportional to the displacement from the reference position. A dc amplifier is used to provide a buffered output.

continued on page 2658